Gravitational Role in Liquid Phase Sintering

Anish Upadhyaya,* Ronald G. Iacocca,** and Randall M. German***

* Director, Materials Development
** Director, Materials Characterization
*** Brush Chair Professor in Materials

P/M Lab, 118 Research West
The Pennsylvania State University
University Park, PA 16802-6809

Abstract

To comprehensively understand the gravitational effects on the evolution of both the microstructure and the macrostructure during liquid phase sintering, W-Ni-Fe alloys with W content varying from 35 to 98 wt.% were sintered in microgravity. Compositions that slump during ground-based sintering also distort when sintered under microgravity. In ground-based sintering, low solid content alloys distort with a typical elephant-foot profile, while in microgravity, the compacts tend to spheroidize. This study shows that microstructural segregation occurs in both ground-based as well as microgravity sintering. In ground-based experiments, because of the density difference between the solid and the liquid phase, the solid content increases from top to the bottom of the sample. In microgravity, the solid content increases from periphery to the center of the samples. This study also shows that the pores during microgravity sintering act as a stable phase and attain anomalous shapes.

Introduction

Liquid phase sintering (LPS) is a common process for the fabrication of dense, net-shape structures. Despite extensive industrial use, several processing difficulties trace to gravity. One easily recognized problem is solid-liquid separation. Like sand settling in water, differences in densities between the solid and liquid phases induce microstructure and compositional segregation. Consequently, only alloys with small quantities of liquid are fabricated on Earth. The tungsten heavy alloys (W-Ni-Fe or W-Ni-Cu) are particularly sensitive to gravitational effects since the liquid-solid density difference is nearly 9 g/cm^3. In this research, we have documented that after sintering on Earth there is a significant gradient in grain coordination number, grain size, grain shape, and solid phase contiguity with the position in the compact. Further, there is a slight difference in grain size due to the compressive stresses during Earth-based sintering. Grain coalescence occurs at gravity induced contacts, giving gradients from the stress in the microstructure due to gravity. It was on the basis of these observations that microgravity and parallel ground-based experiments were performed.

Gravity effects are evident at the macroscale as compact distortion. An excess of liquid causes shape loss, with the formation of the elephant foot geometry or even puddles of solid-liquid. The factors causing distortion in LPS are not understood.

Previous work suggested that it was simply due to the solid-liquid ratio; however, experiments have produced compacts with more than 60 vol.% liquid that retain shape. Compositions that slump on Earth also distorted in microgravity, but in the latter case they spheroidized. Our analysis and modeling efforts now explain distortion during sintering (from both gravitational and surface tension stresses, thus is applicable to both ground-based and microgravity samples) as arising from three features - solid-liquid ratio, dihedral angle, and solubility change when the liquid forms.

Microgravity LPS experiments have been performed in recent years, and the Penn State research team was involved in analysis of samples form flights starting in 1992 (SLJ, IML-2, MSL-1, and MSL-1R). Each investigator has adopted different questions, compositions, and sample preparation techniques. Although each study provides insight, a unified view is missing. Therefore, one goal of the research was to perform cross-study experiments where these various alloys will be processed under similar conditions. This showed the lack of care in prior sample preparation greatly affected the findings and compromised final conclusions. Further, reports from ground-based experiments often proved inadequate to fully document sintering and microstructure findings. One success was the stability of the Large Isothermal Furnace and the support hardware. No malfunction of the flight hardware directly involved in the liquid phase sintering experiments was encountered in microgravity. In this regard, the original plan to use microgravity experiments to isolate gravitational effects on microstructure evolution during liquid phase sintering was very successful. The contrast and comparison of ground-based and microgravity samples, processed from the same powders, in the same furnace, using the same cycles provided the needed separation of variables. Modeling efforts conducted in parallel with the experiments provide a basis for assessing current understanding. The initial phase of the microgravity research was focused on variations in sintering time and solid content using W-Ni-Fe compositions with a constant Ni:Fe ratio of 7:3, but varying W content from 35 to 98%. With improved understanding of the LPS system, we were successful in extending the flight samples to new composition regions with high liquid contents.

Experimental Procedure

Table I summarizes the compositions W-Ni-Fe and W-Ni-Cu alloys used for this investigation. The tungsten heavy alloy samples were cold isostatically pressed, presintered, and then dry-machined in the form of cylindrical pellets of height and diameter 8.29 ± 0.02 mm. The dimensions were so chosen that in case of subsequent sintering performed under microgravity, the compact should not have any constraint on spheroidization. The machined samples were placed in individual alumina crucibles. Samples were grouped in sets of seven, as they had to be sintered under identical conditions. The crucibles were so designated that the bottom of one acted as the top of other. Each set of seven crucibles (with sample in it) were then placed in a BN cartridge tube which was then sealed with a screw cap. The BN ampoule was enclosed in a triple layered Ta tubing. The inner surface of each Ta containment tube is coated with a thin layer of alumina to protect the Ta from attacks by vapors from the sample. All Ta containers were evacuated and sealed using electron beam welding.

Table I. Summary of the compositions used for the MSL-1 experiments.

Cartridge One, 1 min at 1500°C
Cartridge Three, 180 min at 1500°C
Cartridge Four, 600 min at 1500°C

sample number	composition, wt%
1	78W-15.4Ni-6.6Fe
2	65W-24.5Ni-10.5Fe
3	50W-35Ni-15Fe
4	35W-45.5Ni-19.5Fe
5	88W-9.6Ni-2.4Cu
6	88W-7.2Ni-4.8Cu
7	50W-30Ni-20Cu

Cartridge Two, 45 min at 1500°C

sample number	composition, wt%
1	78W-15.4Ni-6.6Fe
2	50W-40Ni-10Cu
3	50W-35Ni-15Fe
4	35W-45.5Ni-19.5Fe
5	88W-9.6Ni-2.4Cu
6	88W-7.2Ni-4.8Cu
7	50W-30Ni-20Cu

Cartridge Five, 120 min at 1500°C

sample number	composition, wt%	preparation
1	78W-15.4Ni-6.6Fe	hot isostatic pressed
2	78W-15.4Ni-6.6Fe	argon presinter
3	78W-15.4Ni-6.6Fe	green cold isostatic pressed
4	78W-15.4Ni-6.6Fe	hydrogen presinter
5	93W-4.9Ni-2.1Fe	green die pressed
6	78W-15.4Ni-6.6Fe	vacuum presinter
7	78W-15.4Ni-6.6Fe	liquid phase sintered

The presintered and machined W-Ni-Fe samples were liquid phase sintered at 1500°C for duration ranging from 1 to 600 min in a Large Isothermal Furnace (LIF)

supplied by Ishikawajima-Harima Heavy Industries Co. Ltd. (IHI) under a collaborative agreement with the National Space Development Agency of Japan (NASDA). Two sets of samples, each with five cartridges, were prepared. One set was for the microgravity experiments, while parallel ground-based experiments were conducted on the second set of samples.

The microgravity sintering experiments were performed aboard the space shuttle *Columbia* as a part of the Microgravity Space Lab 1 and 1R (STS 83 and STS94 missions, respectively) in April 1997 and July 1997. After the samples were sintered, the ground and flight samples were analyzed, and the results were documented in accordance with a well-established protocol. The sintered samples were then quantified using a coordinate measuring machine for distortion and were subsequently sectioned for metallography. The data obtained from these experiments, in combination with parallel Earth-based experiments, provided insight into the effects of gravity on both macrostructural and microstructural development.

Results

All the experiments were successfully completed and met scheduled timeline requirements. Figures 1a and 1b compare the distortion W-Ni-Fe alloys with different liquid volume fractions sintered in ground-based (1g) and microgravity (μg) for 120 min. Prior to sintering, the alloys were presintered at 1400°C for 1 h to nearly full density. Note that slumping decreases with increasing solid (tungsten) volume fraction. The 93W or 98 wt.% W did not slump. Samples containing less than 93 wt.% W distort during both 1g as well as μg sintering. An interesting point to note is that the composition that did not slump during ground-based (1g) sintering, retained their shapes even when sintered in μg.

Ideally, a high liquid content alloy when sintered in μg will try to minimize its energy by attaining a spherical shape. Figure 2a shows the photograph of a 78W-15.4-6.6Fe alloy liquid phase sintered at 1500°C in microgravity for 120 min. Prior to liquid phase sintering, the alloy was presintered at 1400°C for 1 h to 100% density in vacuum. During μg sintering, the cylindrical presintered sample underwent reshaping and completely spheroidized. Figure 2b shows the same composition sintered under unconstrained condition on Earth. Note that the alloy when sintered in 1g condition undergoes slumping and attains the characteristic elephant-foot profile.
Figures 3a and 3b show the photographs from the from the periphery and the center region of the μg sintered 78W samples. Similarly, Figures 3c and 3d show the micrographs from the top and the bottom region of the 1g sintered 78W alloy. Evidently, the alloys sintered in both 1g and μg conditions show microstructural gradients. The degree of segregation, θ, in the microstructure was quantified using following expression:

$$\theta = \frac{X_P^{max} - X_P^{min}}{\sum_{i=1}^{N} X_P^i} N \qquad (1)$$

where P is the locally measured mean attribute (e.g. grain size, solid content, connectivity, or contiguity), and R is the range of the measured variation, which is the difference between the maximum and the minimum numerical value for that attribute.

(a)

(b)

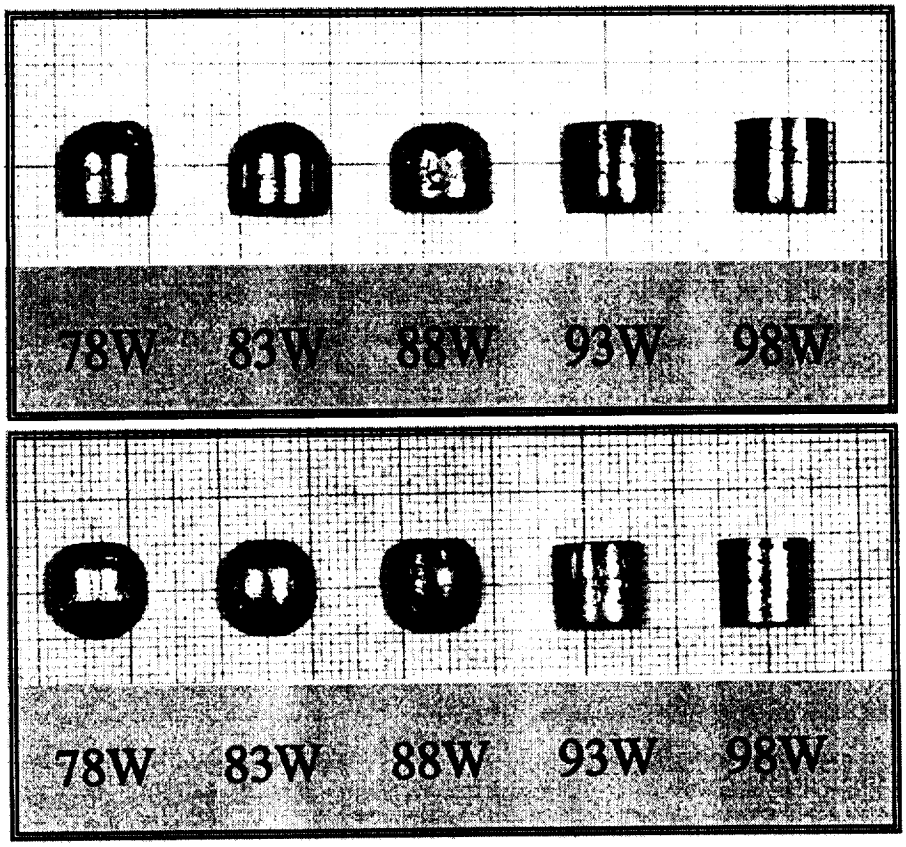

Figure 1. Photograph of W-Ni-Fe alloys with varying W content after liquid phase sintering at 1500°C for 120 min in (a) ground-based and (b) microgravity condition.

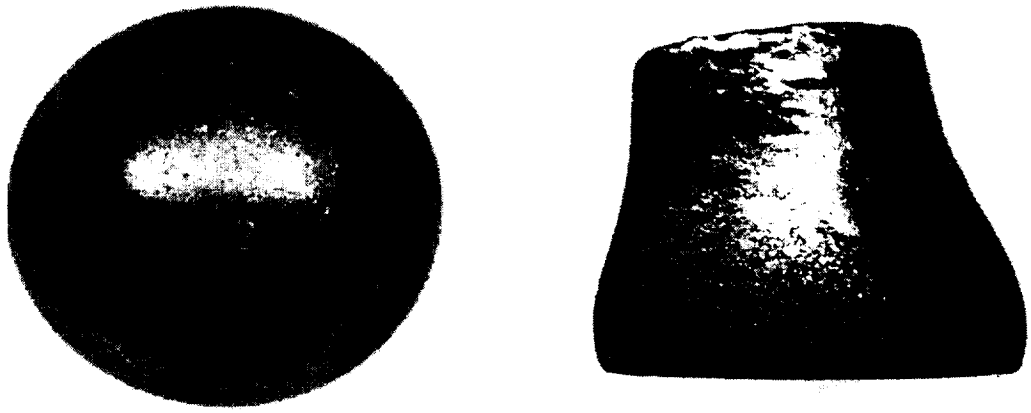

(a) (b)

Figure 2. Shape distortion in 78W-15.4Ni-6.6Fe alloy liquid phase sintered at 1500°C for 120 min in (a) microgravity and (b) ground-based condition.

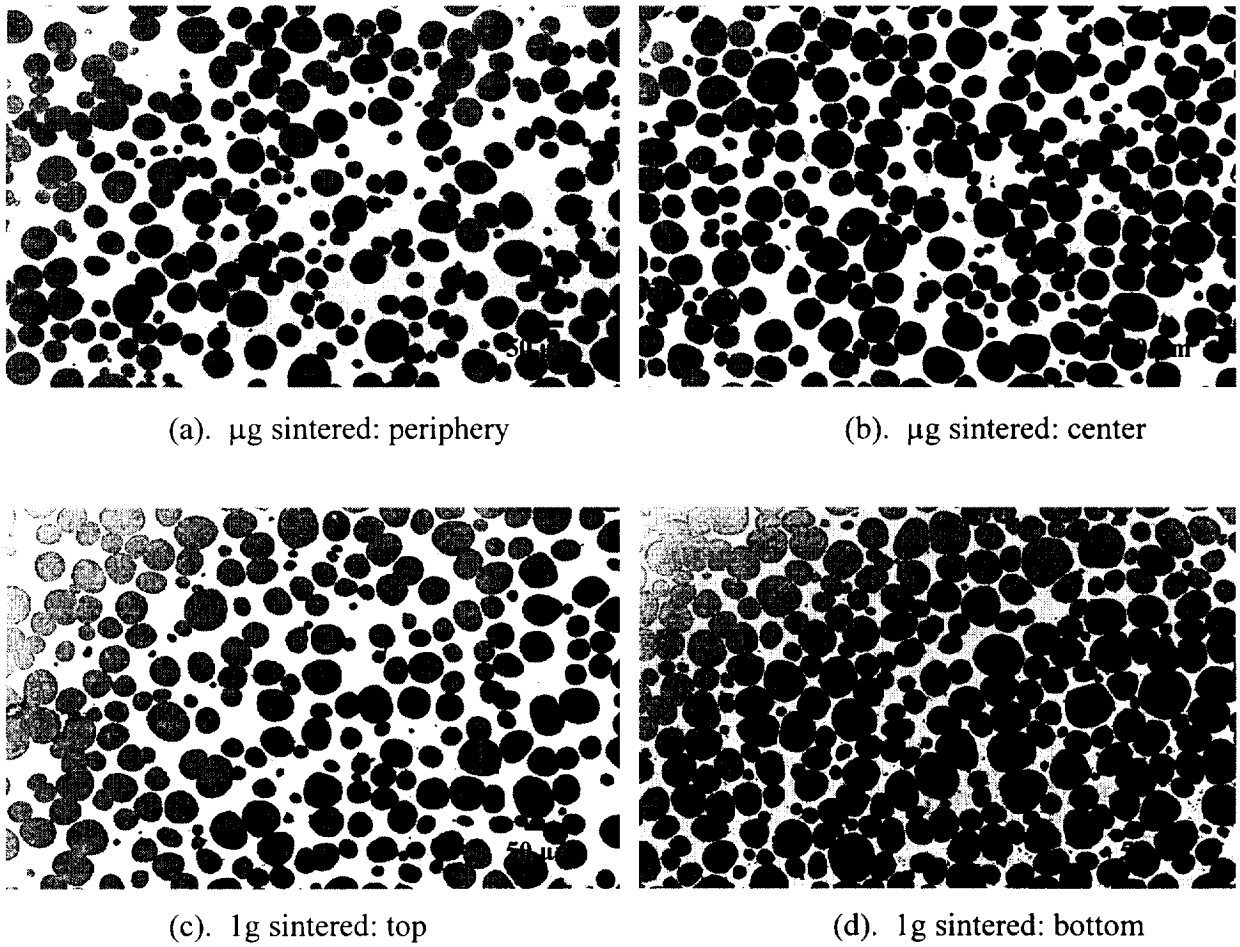

(a). μg sintered: periphery (b). μg sintered: center

(c). 1g sintered: top (d). 1g sintered: bottom

Figure 3. Optical micrographs showing microstructure at various regions of a 78W-15.4Ni-6.6Fe alloy sintered under microgravity (μg) and ground-based (1g) environment.

The range is normalized by the average value to yield a dimensionless measure of segregation.

The corresponding degree of segregation in the 1g and μg sintered 78W alloy- as calculated from Equation 1- is presented in Table II. An interesting fact that comes to light is that microstructural segregation is prevalent in both 1g and μg sintered alloys.

Under microgravity conditions, the pores proved unexpectedly stable and showed anomalous faceting and distorted morphologies. Figure 4a shows a spherical pore in a the center of a 78W alloy liquid phase sintered at 1500°C for 180 min. Figure 4b is an example of a an irregular dog-bone pore that is apparently pinned into a highly distorted shape by tungsten grains. Figures 4c and 4d are scanning electron micrographs showing several grains coalescing and entrapping liquid with a pore inside the grain loop. Figures 5a and 5b compare the pore location in a liquid phase sintered 78W alloy in ground-based and microgravity. Note that when sintered on Earth the pores are located at the top of the sample, where as in microgravity the pores are localized at the center of the sample.

Table II. Influence of gravity on the degree of microstructural segregation, θ, for 78W-15.4Ni-6.6Fe alloy liquid phase sintered at 1500°C for 120 min.

Property	Degree of Segregation, θ	
	ground-based	microgravity
solid content, V_S	0.35	0.47
grain size, $\overline{G}$	0.27	0.96
connectivity, C_g	0.75	0.62
contiguity, C_c	0.38	0.78

Discussion

On comparing the macrostructure the W-Ni-Fe alloys sintered on Earth *versus* that sintered in microgravity, one finds that compositions that distort in 1g sintering undergo distortion when sintered in μg. However, the distorted shapes differ from each other. The low solid content (<60 vol.%) solid alloys attain a typical elephant-foot shape on Earth, whereas in microgravity, the compacts tend to reshape into a spheres. This suggests a link between the microstructural segregation and distortion. In systems with large density difference between the solid and the liquid phase, gravity-induced grain settling increases the packing coordination number at the bottom of the compact. A larger packing coordination number will subject the grains at the bottom to self-compressive stresses, which will cause accelerate slumping.

The microstructure of the ground-based sintered alloys show gradient in the microstructural attributes along the gravity vector. An intriguing feature however was the observance of microstructural segregation even under microgravity. For instance, in the spheroidized 78W-15.4Ni-6.6Fe alloy, the solid content, contiguity, grain size, and connectivity increased from the periphery to the center of the compact. The movement of solid grains in the solid-liquid mixtures can be induced by the shear stress as a result of reshaping event from cylinder to a sphere under the action of surface tension. This reshaping of the compacts from cylinder into a sphere indicates that viscous flow occurred even under the small surface tension forces that act on the samples during microgravity. Compact spheroidization results in the minimization of the gradients in these surface tension forces. Aside from this, the microstructural segregation in microgravity can also lead to spheroidization. The microstructure of the microgravity sintered W-Ni-Fe compact shows an increasing liquid content as we approach towards the periphery. A high liquid content at the periphery will in turn reduce the resistance to flow and promote reshaping and preferential deformation of the peripheral region. To explain microstructural segregation in microgravity, a model based on the total energy of the system has recently been proposed by us. The model calculations suggest that agglomeration and bonding lower system energy and are therefore energetically favored. Thus, a weak agglomeration tendency is inherent in liquid phase sintered systems.

The microstructural examination of the liquid phase sintered W-Ni-Fe sample show a lack of pore buoyancy in microgravity conditions. The lack of buoyancy restricts

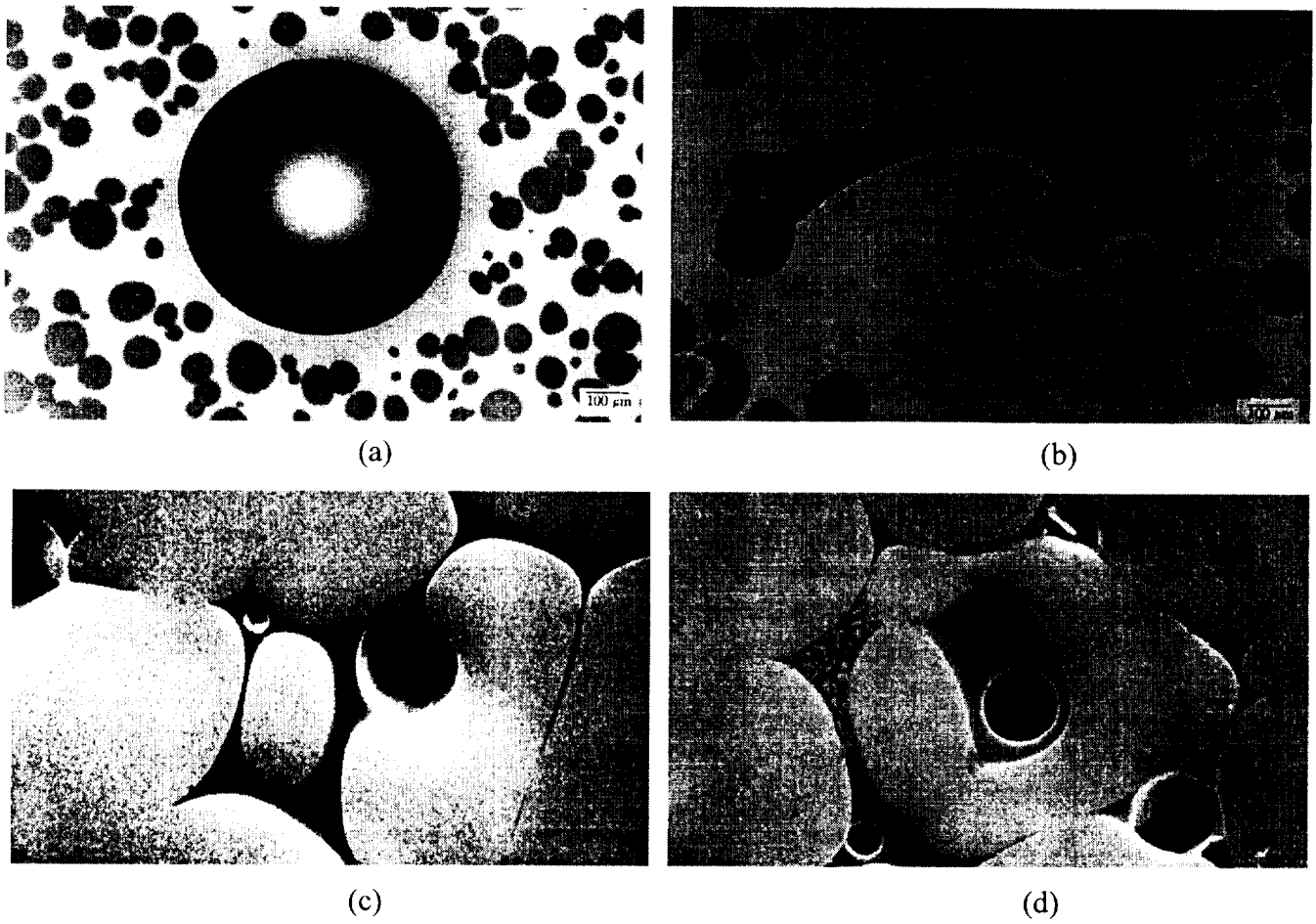

Figure 4. Anomalous pore structures in microgravity sintered 78W-15.4Ni-6.6Fe alloy.

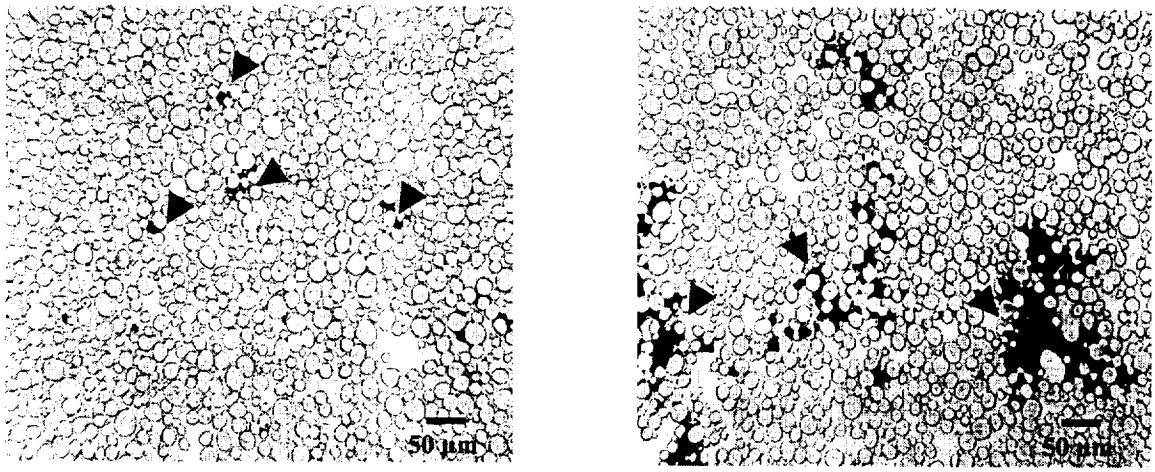

(a). 1g sintered: top

(b). μg sintered: bottom

Figure 5. Porosity in the 78W-15.4Ni-6.6Fe alloy sintered at 1500°C for 180 min under (a) ground-based and (b) microgravity condition.

pore migration and makes the pore as a stable phase. The stable pores caused solid-grain distortion, which indicates a contact angle equilibrium more complex than that treated by Young's equation. Liu and German observed that under microgravity the solid-liquid-vapor equilibrium significantly differs from that observed in the presence of gravity. They found discrepancy in Gibb's analysis of surface energy balance (Young's equation) which did not include the gravity term in the treatment, consequently, Young's equation is not suitable for μg condition.

Conclusions

This research shows important aspects concerning liquid phase sintering on Earth and under microgravity conditions. This study investigates the role of gravity on microstructural evolution and compact shape retention. The results indicate that samples that distort in ground-based sintering undergo distortion in microgravity. In the former, distortion is accompanied by solid-liquid segregation and formation of a typical elephant-foot profile, whereas, in the latter the compacts tend to spheroidize. This proves that the conditions that cause the loss in structural rigidity prevail even in a microgravity environment. The current study shows that during ground-based sintering, gravitational segregation increases with an increasing solid-liquid density difference. Consequently, microstructural links are used to predict the degree of grain settling in dilute alloys sintered in Earth. Microstructural investigation of microgravity sintered W-Ni-Fe alloys disprove the premise that absence of gravity will lead to homogeneous microstructure during sintering. Low solid content alloys, when sintered in microgravity, exhibit microstructural gradients from periphery to the center of the compact. These results suggest that agglomeration is a natural event, even in microgravity. The microstructure also points out to lack of buoyancy-induced pore migration during microgravity sintering.

Summary of Key Findings

A universal grain size distribution for LPS materials has been isolated and described mathematically, and this distribution agrees with recent independent findings. The volume fraction of liquid has been mathematically linked to the grain growth rate constant and solid-liquid density difference for LPS materials, giving the first universal coarsening law applicable to the solid contents characteristic of LPS.

A model has been created for slumping and distortion during LPS. This model describes the role of gravity, component size, substrate friction, and surface tension on reshaping processes. Analysis has shown an important role of grain connectivity and dihedral angle on shape preservation during LPS. Evidence exists that grain boundary wetting by newly formed liquid is a key factor in distortion.

Grain agglomeration has been predicted and observed in dilute solid content systems. The weak agglomeration force was first modeled for LPS, but may be applicable to many situations including solid-liquid, liquid-liquid, solid-vapor, and liquid-vapor systems. The agglomeration event was observed in microgravity samples sintered by Kohara and Ekbom.

Based on pore stabilities in the microgravity samples, we have revisited the derivation of Young's equation and found Gibbs' original treatment is incorrect since a gravity term was dropped from the derivation.

Coalescence has been documented in a zero dihedral angle LPS system conclusively to prove Ostwald ripening theories are incorrect in ignoring this effect. Further, grain rotation as part of coalescence has been measured during long time LPS. Electron channeling experiments will show the emergence of preferred grain orientations for coalescence during long term LPS.

Early evidence shows a non-random radial distribution function in the grain size of LPS heavy alloys.

The settled region of Earth-based LPS samples has been analyzed for the density difference effect and the terminal skeletal structure for no solid-liquid density difference. A model for the solid content versus position in the settled solid structure accurately explains all previous observations.

A new generalized idea of grain coordination number versus effective pressure has emerged that may have applicability to loosely packed particles. The model expresses the mean coordination number as a function of the effective pressure. Ground-based experiments are being performed to test this model.

Pore structure observations in microgravity LPS samples show a high stability. This suggests buoyancy may be important to densification during LPS on Earth. A complication is the lack of a reducing atmosphere during microgravity sintering, but under identical ground-based LIF experiments a gravity role is evident.

Acknowledgement

The funding for this research was provided by the National Aeronautical and Space Administration (NASA). Data from these experiments are available by accessing the P/M Lab website at http://pmlab.esm.psu.edu/pmhome.htm.

Some Publications for In-Depth Study

1. C. M. Kipphut, A. Bose, S. Farooq and R. M. German, "Gravity and Configurational Energy Induced Microstructural Changes in Liquid Phase Sintering," *Metallurgical Transactions A*, 1988, vol. 19A, pp. 1905-1913.
2. R. M. German and S. Farooq, "An Update on the Theory of Liquid Phase Sintering," *Sintering '87,* vol. 1, S. Somiya, M. Shimade, M. Yoshimura, and R. Watanabe (eds.), Elsevier Applied Science, London, UK, 1989, pp. 459-464.
3. S. C. Yang, S. S. Mani and R. M. German, "The Effect of Contiguity on Growth Kinetics in Liquid Phase Sintering," *JOM*, 1990, vol. 42, no. 5, pp. 16-19.
4. S. C. Yang and R. M. German, "Gravitational Limit of Particle Volume Fraction in Liquid Phase Sintering," *Metallurgical Transactions A*, 1991, vol. 22A, pp. 786-791.
5. S. S. Mani and R. M. German, "Gravitational Effects on Microstructural Parameters During Liquid Phase Sintering," Advances in Powder Metallurgy, 1991, vol. 4, Metal Powder Industries Federation, Princeton, NJ, pp. 195-212.
6. S. C. Yang and R. M. German, "Generic Grain Size Distribution for Liquid Phase Sintering," *Scripta Metallurgica*, 1992, vol. 26, pp. 95-98.
7. R. M. German, A. Bose and S. S. Mani, "Sintering Time and Atmosphere Influences on the Microstructure and Mechanical Properties of Tungsten Heavy Alloys," *Metallurgical Transactions A*, 1992, vol. 23A, pp. 211-219.

8. R. G. Iacocca and R. M. German, "Experimental Design for Liquid Phase Sintering in Microgravity," Advances in Powder Metallurgy and Particulate Materials, 1993, vol. 2, Metal Powder Industries Federation, Princeton, NJ, pp. 181-194.
9. R. M. German, "Microstructure of the Gravitationally Settled Region in a Liquid Phase Sintered Dilute Tungsten Heavy Alloy," *Metallurgical Materials Transactions A*, 1995, vol. 26A, pp. 279-288.
10. R. Raman and R. M. German, "A Mathematical Model for Gravity-Induced Distortion During Liquid Phase Sintering," *Metallurgical Materials Transactions A*, 1995, vol. 26A, pp. 653-659.
11. Y. Liu, D. F. Heaney and R. M. German, "Gravitational Effects on Solid Grain Packing in Liquid Phase Sintering," Tungsten and Refractory Metals, A. Bose and R. Dowding (eds.), Metal Powder Industries Federation, Princeton, NJ, 1995, pp. 121-128.
12. Y. Liu, D. F. Heaney and R. M. German, "Gravity Induced Solid Grain Packing during Liquid Phase Sintering," *Acta Metallurgica Materialia*, 1995, vol. 43, pp. 1587-1592.
13. R. M. German, R. G. Iacocca, J. L. Johnson, Y. Liu and A. Upadhyaya, "Liquid-Phase Sintering Under Microgravity Conditions," *JOM*, 1995, vol. 47, no. 8, pp. 46-48.
14. Y. Liu, R. Iacocca, J. L. Johnson, R. M. German, and S. Kohara, "Microstructural Anomalies in a W-Ni Alloy Liquid Phase Sintered under Microgravity Conditions," *Metallurgical Materials Transactions A*, 1995, vol. 26A, pp. 2485-2486.
15. R. G. Iacocca, Y. Liu, and R. M. German, "Microstructural Examination of Tungsten Heavy Alloys Sintered in a Microgravity Environment," Advances in Powder Metallurgy and Particulate Materials, 1995, vol. 1, pp. 4.239-4.249.
16. D. F. Heaney, R. M. German, and I. S. Ahn, "The Gravitational Effects on Low Solid-Volume Fraction Liquid-Phase Sintering," *Journal Materials Science*, 1995, vol. 30, pp. 5808-5812.
17. Y. Liu and R. M. German, A Relationship Between Contact Angle and Surface Tensions, Sintering 1995, R. M. German, G. L. Messing, and R. Cornwall (eds.), Marcel Dekker, New York, NY, 1996, pp. 229-236.
18. R. M. German, "Grain Agglomeration in Solid-Liquid Mixtures Under Microgravity Conditions," *Metallurgical Materials Transactions B*, 1995, vol. 26B, pp. 649-651.
19. Y. Liu and R. M. German, "Contact Angle and Solid-Liquid-Vapor Equilibrium," *Acta Materialia*, 1996, vol. 44, pp. 1657-1663.
20. R. M. German and Y. Liu, "Grain Agglomeration in Liquid Phase Sintering," *Journal Material Synthesis Processing*," 1996, vol. 4, pp. 23-34.
21. J. L. Johnson and R. M. German, "A Solid-State Contributions to Densification during Liquid Phase Sintering," *Metallurgical Materials Transactions B*, 1996, vol. 27B, pp. 901-909.
22. A. Upadhyaya and R. M. German, "Control of Distortion during Liquid Phase Sintering," Proceedings of 14th International Plansee Seminar-1997, vol. 2, G. Keneringer, P. Rödhammer, and P. Wilhartitz (eds.), Plansee AG, Reutte, Austria, 1997, pp. 68-85.
23. A. Upadhyaya and R. M. German, "Densification and Distortion in Liquid Phase Sintered W-Cu Alloys," *International Journal Powder Metallurgy*, 1998, vol. 34, pp. 43-55.

24. . J. L. Johnson, A. Upadhyaya, and R. M. German, "Microstructural Effects on Distortion and Solid-Liquid Segregation during Liquid Phase Sintering under Microgravity Conditions," *Metallurgical Materials Transactions B*, 1998, vol. 29B, pp. 857-866.
25. A. Upadhyaya and R. M. German, "Shape Distortion in Liquid Phase Sintered Tungsten Heavy Alloys," *Metallurgical Materials Transactions A* (in press)
26. A. Upadhyaya, "A Microstructure-Based Model for Shape Distortion during Liquid Phase Sintering," *Ph.D. Thesis*, The Pennsylvania State University, University Park, PA, 1998.